72-1008

HOLTEC INTERNATIONAL

Holtec Center, 555 Lincoln Drive West, Marlton, NJ 08053

Telephone (856) 797-0900
Fax (856) 797-0909

August 4, 2000

U.S. Nuclear Regulatory Commission
ATTN: Document Control Desk
Washington, DC 20555-0001

Subject: NRC 10 CFR 72 Certificate of Compliance No. 1008
License Amendment Request 1008-2

References:
1. Holtec Project No. 5014
2. Holtec Topical Safety Analysis Report No. HI-941184, Proposed Revision 11.
3. Holtec License Amendment Request 1008-1, dated November 24, 1999 (as supplemented)

Dear Sir:

In accordance with 10 CFR 72.244, Holtec International hereby submits License Amendment Request (LAR) 1008-2, proposing changes to 10 CFR 72 Certificate of Compliance (CoC) No. 1008 for the HI-STAR 100 System. The description of the changes, reason for the changes, and justification for the changes are provided below. In preparing this amendment request package, we have included marked-up and final versions of the CoC and proposed Topical Safety Analysis Report (TSAR) changes to assist the staff in their review. Please note that these changes pivot primarily around TSAR Appendix 3.A. Therefore, while certain other proposed TSAR changes are provided on a page basis, an entire replacement of Appendix 3.A is provided for your review.

This LAR proposes a change to Appendix B of the CoC, to modify the verbiage applicable to ISFSI pad design to better serve our utility clients, while retaining the same design bases and safety margins. These proposed changes are being requested in light of the concrete in certain parts of the 24-inch thick ISFSI pads at Commonwealth Edison (ComEd) Company's Dresden Nuclear Power Station (DNPS), Unit 1 exceeding the maximum 28-day compressive strength of 4,200 psi currently allowed by the CoC. Approval of these proposed changes is requested to permit placement of HI-STAR 100 and HI-STORM 100 dry storage casks on the balance of the DNPS, Unit 1 ISFSI[1] pads. This change is also generic in nature in that it provides the flexibility for all of our utility customers to design site-specific ISFSI pads, with the restriction that the 60-g design basis cask deceleration limit must not be exceeded under all design basis cask drop and tip-over scenarios.

[1] A similar change will be included in our upcoming HI-STORM License Amendment Request 1014-1 supplement currently scheduled for submittal by August 31, 2000.

NMSS01 Public

HOLTEC INTERNATIONAL

Holtec Center, 555 Lincoln Drive West, Marlton, NJ 08053

Telephone (856) 797-0900
Fax (856) 797-0909

Description of Proposed Changes

a. Revise CoC 1008, Appendix B, Section 1.4.6 as shown in Attachment 1 to remove the specific ISFSI pad and subgrade design parameters. Insert a single requirement for all ISFSI pads, including the subgrade, to be designed such that all design basis cask drop and tipover events on the pad result in a cask deceleration less than 60 g's at the top of the fuel basket when analyzed using a methodologies consistent with those described in the HI-STAR 100 TSAR.

b. Revise TSAR Sections 2.2.3.2 and 3.4.9, Table 2.2.9, and Appendix 3.A as shown in Attachment 2 to: 1) conform with the above change to the CoC and 2) to provide a second set of "pre-qualified" ISFSI pad and subgrade design parameters for which an analysis has been performed that confirms all design basis drop and tipover events result in cask deceleration levels less than the design basis 60-g limit.

c. Revise TSAR Appendix 3.A to delete the miscellaneous numerical calculations and Figures 3.A.20 through 3.A.31.

Reason for Proposed Changes

a and b. The current CoC requires that all ISFSI pads be designed to meet a single set of design parameters, including pad thickness, concrete compressive strength, reinforcing bar yield strength, and subgrade modulus of elasticity. This proposed CoC change allows the necessary flexibility for utility licensees to design their ISFSI pads according to their site-specific needs and geological characteristics, while still meeting the design basis cask deceleration limit. The addition of a second set of acceptable ISFSI pad parameters to the TSAR provides two pre-approved sets of parameters utilities may choose to use in lieu of a performing a site-specific design and analysis.

c. The information being deleted from TSAR Appendix 3.A is at a level of detail which is more appropriate for inclusion in a calculation package rather than the TSAR.

Justification for Proposed Changes

a and b. The deceleration limit of 60-g's for the HI-STAR 100 System provides assurance that the cask system, including contents, will remain intact and retrievable after a postulated drop event and a non-mechanistic tip-over event. Therefore, the 60-g

HOLTEC
INTERNATIONAL

Holtec Center, 555 Lincoln Drive West, Marlton, NJ 08053
Telephone (856) 797-0900
Fax (856) 797-0909

deceleration limit is the appropriate safety limit to be included in the CoC, while the specific ISFSI pad design parameters may be left to the discretion of the general licensee. The stiffness of the ISFSI pad and subgrade upon which the cask is postulated to drop are key inputs to the structural analyses.

To assist the licensee in designing their pads, Holtec has analyzed a second set of ISFSI design parameters, using the approved TSAR methodologies for cask drop and tip-over events, as part of these proposed changes. However, provided licensees employ the same analysis methodologies, it is acceptable for them to design their ISFSI pads using *any* combination of design parameters that results in a structurally competent pad for which cask decelerations limits are shown to be met.

c. The information being removed from TSAR Appendix 3.A will be maintained in an internal Holtec calculation package. Changes to this information will be controlled under the Holtec QA program, which requires technical and QA reviews of all changes to calculation packages. Should such changes cause a change to the information remaining in the TSAR, those changes would be subject to evaluation and approval under the 10 CFR 72.48 process.

We are requesting NRC approval of this proposed CoC amendment by March, 2001 to support ComEd's schedule for placing additional HI-STAR 100 and HI-STORM 100 dry storage casks on the DNPS, Unit 1 ISFSI pads.

We understand that the rulemaking process will be initiated shortly to incorporate changes to the HI-STAR 100 CoC and TSAR that we requested in November, 1999 (Ref. 3). Therefore, our proposed CoC and TSAR changes in this LAR are written against our November, 1999 proposed revised CoC and TSAR for consistency. We realize, or course, that this request will be handled as a separate licensing action.

HOLTEC INTERNATIONAL

Holtec Center, 555 Lincoln Drive West, Marlton, NJ 08053

Telephone (856) 797-0900
Fax (856) 797-0909

If you have any questions or require additional information, please contact us.

Sincerely,

Brian Gutherman, P.E.
Licensing Manager

Approved:

K. P. Singh, Ph.D., P.E.
President and CEO

Document I.D.: 5014397

Attachments: 1: Proposed Changes to CoC 1008, Appendix B (mark-up and final versions – 5 pages)
2: Proposed changes to HI-STAR TSAR (38 pages)

Cc: Ms. Virginia Tharpe, USNRC, (10 hard copies, w/attachments and floppy disk of cover letter and Attachment 1)

Mr. E. W. Brach, USNRC (cover letter only)
Ms. S. Frant-Shankman, USNRC (cover letter only)
Mr. Eric Leeds, USNRC (cover letter only)
Mr. J. Nathan Leech, ComEd (w/attach.)
Mr. Ken Ainger, ComEd, (w/attach.)

Technical Concurrence:

Dr. Alan Soler (Structural Evaluation)

HOLTEC INTERNATIONAL

Holtec Center, 555 Lincoln Drive West, Marlton, NJ 08053

Telephone (856) 797-0900
Fax (856) 797-0909

Distribution (w/o attach.) :

Recipient	Affiliation
Mr. Jim Wade	Southern Nuclear Operating Company
Mr. Robert Berryhill	Southern Nuclear Operating Company
Mr. Kenneth Phy	New York Power Authority
Dr. Max DeLong	Private Fuel Storage
Mr. Stan Miller	Vermont Yankee Nuclear Power Corporation
Mr. David Larkin	Energy Northwest
Mr. Bruce Patton	Pacific Gas & Electric – Diablo Canyon
Mr. Mark Smith	Pacific Gas & Electric – Humboldt Bay
Mr. Terry Grebel	Pacific Gas & Electric
Mr. Roger Johnson	Pacific Gas & Electric
Mr. Charles Davis	Tennessee Valley Authority – Sequoyah Plant
Mr. Rodney Pickard	American Electric Power
Mr. Eric Meils	Wisconsin Electric Power Company
Mr. Paul Plante	Maine Yankee Atomic Power Company
Mr. Robert Ashe-Everest	Southern California Edison
Mr. Darrell Williams	Entergy Operations – Arkansas Nuclear One
Mr. Chris Kudla	Entergy Operations – Millstone Unit 1 Decommissioning
Mr. Charles Minnot	Entergy Operations – Pilgrim Station
Mr. Vee Dunn	Entergy Operations – Grand Gulf Station
Ms. Jodi Furr	Entergy Operations – River Bend Station
Mr. Ben Garrett	GPUN – Oyster Creek Nuclear Power Station
Mr. Brian Wohlers	Alliant Energy
Mr. William Swantz	Nebraska Public Power District
Mr. Gary Krieser	Nuclear Management Company
Mr. Matt Eyre	PECO Energy
Mr. Al Gould	Florida Power & Light
Dr. Seymour Raffety	Dairyland Power
Mr. John Sanchez	Consolidated Edison Company
Ms. Kathy Picciott	Niagara Mohawk Power Corporation
Mr. John Donnell	Private Fuel Storage, LLC (SWEC)
Mr. Steve Edwards	Carolina Power and Light
Mr. Simon Hseih	Detroit Edison
Mr. Rick Scofield	Omaha Public Power District
Dr. Stanley Turner	Holtec International, Florida Operations Center

HOLTEC INTERNATIONAL

Holtec Center, 555 Lincoln Drive West, Marlton, NJ 08053

Telephone (856) 797-0900
Fax (856) 797-0909

U.S. Nuclear Regulatory Commission
ATTN: Document Control Desk
Document ID 5014397
Attachment 1
5 total pages, including this page

PROPOSED COC 1008 CHANGES (MARK-UP AND FINAL VERSIONS)

2. The allowed temperature extremes, averaged over a three day period, shall be greater than -40°F, and less than 125°F.

3. The horizontal and vertical seismic acceleration levels are bounded by the values listed below in Table 1-4.

Table 1-4

Design-Basis Earthquake Input on the Top Surface of an ISFSI Pad

Horizontal g-level in each of two orthogonal directions	Horizontal g-level Vector Sum	Corresponding Vertical g-level (upward)
0.222 g	0.314 g	1.00 x 0.222 g = 0.222 g
0.235 g	0.332 g	0.75 x 0.235 g = 0.176 g
0.24 g	0.339 g	0.667 x 0.24 g = 0.160 g
0.25 g	0.354 g	0.500 x 0.25 g = 0.125 g

4. The analyzed flood condition of 12 fps water velocity and a height of 656 feet of water (full submergence of the loaded cask) are not exceeded.

5. The potential for fire and explosion shall be addressed, based on site-specific considerations. This includes the condition that the onsite transporter fuel tank will contain no more than 50 gallons of combustible transporter fuel.

6. *User's ISFSI pads shall be verified by analysis to limit cask deceleration during a design basis drop or non-mechanistic tip-over event to ≤ 60 g's at the top of the MPC fuel basket. Analyses shall be performed using methodologies consistent with those described in the HI-STAR TSAR.* ~~In addition to the requirement of 10 CFR 72.212(b)(2)(ii), the cask storage pads and foundation shall include the following characteristics as applicable to the drop and tipover analyses:~~

~~a. Concrete thickness: ≤ 36 inches~~

~~b. Concrete compressive strength: ≤ 4,200 psi at 28 days~~

~~c. Reinforcement top and bottom (Both Directions):~~
~~Reinforcement area and spacing determined by analysis~~
~~Reinforcing bar shall be 60 ksi yield strength ASTM material~~

~~d. Soil effective modulus of elasticity: ≤ 28,000 psi (Measured prior to ISFSI pad installation)~~

~~An acceptable method of defining the soil modulus of elasticity applicable to the drop and tipover analyses is providedin Table 13 of NUREG/CR-6608 with soil classification in accordance with ASTM-D2487-93, Standard Classification of Soils for Engineering Purposes (Unified Soil Classification System USCS) and density determination in accordance with ASTM D1586-84, Standard Test Method for Penetration Test and Split/Barrel Sampling of Soils.~~

7. In cases where engineered features (i.e., berms, shield walls) are used to ensure that the requirements of 10 CFR 72.104(a) are met, such features are to be considered important to safety and must be evaluated to determine the applicable Quality Assurance Category.

1.5 Design Specifications

1.5.1 Specifications Important for Criticality Control

1.5.1.1 MPC-24

1. Minimum flux trap size: 1.09 in

2. Minimum ^{10}B loading in the Boral neutron absorbers: 0.0267 g/cm^2

1.5.1.2 MPC-68 and MPC-68F

1. Minimum fuel cell pitch: 6.43 in

2. Minimum ^{10}B loading in the Boral neutron absorbers: 0.0372 g/cm^2 in the MPC-68, and 0.01 g/cm^2 in the MPC-68F.

1.5.2 Specifications Important for Thermal Performance

1.5.2.1 OVERPACK

The paint used on the HI-STAR 100 OVERPACK must have an emissivity no less than 0.85.

2. The allowed temperature extremes, averaged over a three day period, shall be greater than -40°F, and less than 125°F.

3. The horizontal and vertical seismic acceleration levels are bounded by the values listed below in Table 1-4.

Table 1-4

Design-Basis Earthquake Input on the Top Surface of an ISFSI Pad

Horizontal g-level in each of two orthogonal directions	Horizontal g-level Vector Sum	Corresponding Vertical g-level (upward)
0.222 g	0.314 g	1.00 x 0.222 g = 0.222 g
0.235 g	0.332 g	0.75 x 0.235 g = 0.176 g
0.24 g	0.339 g	0.667 x 0.24 g = 0.160 g
0.25 g	0.354 g	0.500 x 0.25 g = 0.125 g

4. The analyzed flood condition of 12 fps water velocity and a height of 656 feet of water (full submergence of the loaded cask) are not exceeded.

5. The potential for fire and explosion shall be addressed, based on site-specific considerations. This includes the condition that the onsite transporter fuel tank will contain no more than 50 gallons of combustible transporter fuel.

6. User's ISFSI pads shall be verified by analysis to limit cask deceleration during a design basis drop or non-mechanistic tip-over event to $\leq$ 60 g's at the top of the MPC fuel basket. Analyses shall be performed using methodologies consistent with those described in the HI-STAR TSAR.

7. In cases where engineered features (i.e., berms, shield walls) are used to ensure that the requirements of 10 CFR 72.104(a) are met, such features are to be considered important to safety and must be evaluated to determine the applicable Quality Assurance Category.

1.5 Design Specifications

1.5.1 Specifications Important for Criticality Control

1.5.1.1 MPC-24

1. Minimum flux trap size: 1.09 in

2. Minimum ^{10}B loading in the Boral neutron absorbers: 0.0267 g/cm^2

1.5.1.2 MPC-68 and MPC-68F

1 .
Minimum fuel cell pitch: 6.43 in

2 .
Minimum ^{10}B loading in the Boral neutron absorbers: 0.0372 g/cm^2 in the MPC-68, and 0.01 g/cm^2 in the MPC-68F.

1.5.2 Specifications Important for Thermal Performance

1.5.2.1 OVERPACK

The paint used on the HI-STAR 100 OVERPACK must have an emissivity no less than 0.85.

HOLTEC INTERNATIONAL

Holtec Center, 555 Lincoln Drive West, Marlton, NJ 08053

Telephone (856) 797-0900
Fax (856) 797-0909

U.S. Nuclear Regulatory Commission
ATTN: Document Control Desk
Document ID 5014397
Attachment 2
38 total pages, including this page

PROPOSED TSAR CHANGES

and impulsive loads under accident events such as cask drop and non-mechanistic tip-over are less than those calculated by the dynamic models used in the structural qualifications.

2.2.3.2 Tip-Over

The HI-STAR 100 System is demonstrated to remain kinematically stable under the design basis environmental phenomena (tornado, earthquake, etc.). However, the cask must also withstand impact due to a postulated tip-over event. The structural integrity of a loaded HI-STAR 100 System after a tip-over onto a reinforced concrete pad is demonstrated using a side drop bounding analysis. The cask tip-over is not postulated as an outcome of any environmental phenomenon or accident condition. The cask tip-over is a non-mechanistic event.

During original licensing for the HI-STAR 100 System, a single set of ISFSI pad and subgrade design parameters (now labeled Set A) was established. Experience has shown that achieving a maximum concrete compressive strength (at 28 days) of 4,200 psi can be difficult. Therefore, a second set of ISFSI pad and subgrade design parameters (labeled Set B) has been developed. The Set B ISFSI parameters include a thinner concrete pad and less stiff subgrade, which allow for a higher concrete compressive strength. Cask deceleration values for all design basis drop and tipover events have been verified to be less than or equal to the design limit of 60 g's at the top of the fuel basket for both sets of ISFSI pad parameters.

The original set and the new set (Set B) of acceptable ISFSI pad *and subgrade design parameters* are specified in Table 2.2.9. *Users may design their ISFSI pads and subgrade in compliance with either parameter Set A or Set B. Alternatively, users may design their site-specific ISFSI pad and subgrade using any combination of design parameters which result in a structurally competent pad under provisions of ACI 318 and also limits the deceleration of the cask to less than or equal to 60 g's for the design basis drop and tip-over events. The structural analyses for site-specific ISFSI pad design shall be performed using methodologies consistent with those described in this TSAR, as applicable.*

2.2.3.3 Fire

The possibility of a fire accident near an ISFSI site is considered to be extremely remote due to the absence of significant combustible materials. The only credible concern is related to a transport vehicle fuel tank fire engulfing a cask while it is being moved to the ISFSI.

The HI-STAR 100 System must withstand temperatures due to a fire event. The fire accident for storage is conservatively specified to be the result of the spillage and ignition of 50 gallons of combustible transporter fuel. The HI-STAR overpack surfaces are considered to receive an incident radiation and convection heat flux from the fire. Table 2.2.8 provides the fire duration based on the amount of flammable materials assumed. The temperature of the fire is assumed to be 1475EF in accordance with 10CFR71.73.

Table 2.2.9

EXAMPLES OF ACCEPTABLE ISFSI PAD *DESIGN PARAMETERS*

PARAMETER	***PARAMETER*† *SET 'A'***	***PARAMETER SET 'B'***
Concrete thickness, t_p	≤ 36 inches	*≤ 28 inches*
Concrete Compressive Strength *(at 28 days),* f_c'	≤ 4,200 psi	*≤ 6,000 psi*
Reinforcement Top and Bottom (both directions)	Reinforcing bar shall be 60 ksi Yield Strength ASTM Material	*Reinforcing bar shall be 60 ksi Yield Strength ASTM Material*
Subgrade Effective Modulus of Elasticity†† *(measured prior to ISFSI pad installation), E*	≤ 28,000 psi	*≤ 16,000*

† The characteristics of this pad are identical to the pad considered by Lawrence Livermore Laboratory (see Appendix 3.A).

†† An acceptable method of defining the soil effective modulus of elasticity applicable to the drop and tipover analysis is provided in Table 13 of NUREG/CR-6608 with soil classification in accordance with ASTM-D2487 Standard Classification of Soils for Engineering Purposes (Unified Soil Classification System USCS) and density determination in accordance with ASTM-D1586 Standard Test Method for Penetration Test and Split/Barrel Sampling of Soils.

HI-STAR 100 Missile Impact - Global Stress Results (Load Case 06 in Table 3.1.5)			
Item	Value (ksi)	Allowable (ksi)	Safety Factor
Inner Shell - Side Strike	12.6	48.2	3.83
Intermediate Shell – Side Strike	14.3	39.1	2.73
Top Lid - (End Strike)	48.45	64.6.	1.33

The above summary table does not include the circumferential fabrication stress since these have been designated as self-limiting, and therefore fall into the category of a secondary stress which need not be included in a Level D stress evaluation.

3.4.9 Non-Mechanistic Tip-over, Side and Vertical Drop Events

Pursuant to the provision in NUREG-1536, a non-mechanistic tip-over of a loaded HI-STAR 100 System on to the ISFSI pad is considered. Analyses are also performed to determine the maximum deceleration sustained by a side or vertical free fall of a loaded HI-STAR 100 System onto the ISFSI pad. The object of the analyses is to demonstrate that the plastic deformation in the fuel basket is sufficiently limited to permit the stored SNF to be retrieved by normal means and that there is no significant loss of radiation shielding in the system.

Ready retrievability of the fuel is presumed to be ensured if stress levels in the MPC structure remain below Level D limits during the postulated drop events.

Subsequent to the accident events, the overpack must be shown to contain the shielding so that unacceptable radiation levels do not result from the accident.

Appendix 3.A provides a description of the dynamic finite element analyses undertaken to establish the decelerations resulting from the postulated event. A non-mechanistic tip-over is considered together with a side and end drop of a loaded HI-STAR 100 System. A dynamic finite element analysis of each event is performed using a commercial finite element code well suited for such dynamic analyses with interface impact and non-linear material behavior. This code and methodology have been fully benchmarked against Lawrence Livermore Laboratories test data and correlation [3.4.12].

The table below provides the value of peak computed decelerations at the top of the fuel basket for the non-mechanistic tip-over, vertical drop and side drop scenarios. It is seen that, in all cases, the peak deceleration is under 60 g's.

Scenario	*Maximum Deceleration at Top of Fuel Basket (in g's)*	
	Set A (36" Thick Pad Case)	*Set B (28" Thick Pad Case)*
Non-Mechanistic Tipover	*59.81*	*50.64*
Vertical Drop 21" Free Fall	*52.26*	*50.25*
Side Drop, 72" Free Fall	*49.67*	*46.77*

APPENDIX 3.A: HI-STAR DECELERATION UNDER POSTULATED DROP EVENTS AND TIPOVER

3.A.1 INTRODUCTION

Handling accidents with a HI-STAR overpack containing a loaded MPC are credible events (Section 2.2.3). The stress analyses carried out in Chapter 3 of this safety analysis report assume that the inertial loading on the load bearing members of the MPC, fuel basket, and the overpack due to a handling accident are limited by the Table 3.1.2 decelerations. The maximum deceleration experienced by a structural component is the product of the rigid body deceleration sustained by the structure and the dynamic load factor (DLF) applicable to that structural component. The dynamic load factor (DLF) is a function of the contact impulse and the structural characteristics of the component. A solution for dynamic load factors is provided in Appendix 3.X.

The rigid body deceleration is a strong function of the load-deformation characteristics of the impact interface, weight of the cask, and the drop height. For the HI-STAR 100 System, the weight of the structure and its surface compliance characteristics are known. However, the contact stiffness of the ISFSI pad (and other surfaces over which the HI-STAR 100 may be carried during its movement to the ISFSI) is site-dependent. The contact resistance of the collision interface, which is composed of the HI-STAR 100 and the impacted surface compliances, therefore, is not known a priori for a site. For conservatism, the HI-STAR 100 cask is simulated as a rigid body (infinite surface stiffness) which has the effect of maximizing the stiffness of the contact interface. Analyses for the rigid body decelerations are presented here for a reference ISFSI pad (which is the pad used in a recent Lawrence Livermore National Laboratory report). The surface compliance of the pad, therefore, is the only source of interface deformation in the dynamic simulations considered in this appendix.

An in-depth investigation by the Lawrence Livermore Laboratory (LLNL) into the mechanics of impact between a cask-like impactor on a reinforced concrete slab founded on a soil-like subgrade has identified three key parameters, namely, the thickness of the concrete slab, t_p, compressive strength of the concrete, f_c' and equivalent Young's Modulus of the subgrade, E. These three parameters are key variables in establishing the stiffness of the pad under impact scenarios. The LLNL reference pad parameters, which we hereafter denote as Set A, provide one set of values of t_p, f_c', and E which are found to satisfy the deceleration criteria applicable to the HI-STAR 100 cask. Another set of parameters, referred to as Set B herein, are also shown to satisfy the g-load limit requirements. In fact, an infinite number of combinations of t_p, f_c', and E can be compiled which would meet the g-load limit qualification. However, in addition to satisfying the g-limit criterion, the pad must be demonstrated to possess sufficient flexural and shear stiffness to meet the ACI 318 strength limits under factored load combinations. The minimum strength requirement to comply with ACI 318 provisions places a restriction on the lower bound values of t_p, f_c', and E which must be met in an ISFSI pad design. Our focus in this appendix, however, is to quantify the peak decelerations that would be experienced by a loaded HI-STAR 100 cask under the postulated impact scenarios for two pad designs defined by parameter Sets A and B, respectively. The information

presented in this appendix also serves to further authenticate the veracity of the Holtec DYNA3D model described in the 1997 benchmark report [3.A.4.]

3.A.2 Purpose

The purpose of this appendix is to demonstrate that the rigid body decelerations are sufficiently low so that the design basis deceleration of 60g is not exceeded. Three scenarios of accidental drop of a loaded HI-STAR 100 cask on the ISFSI pad are considered in this appendix. They are:

i. Side drop: A loaded HI-STAR 100 free-falls in a horizontal orientation (casks's axis is horizontal) from a height "h" before impacting the ISFSI pad.

ii. Tipover: A loaded HI-STAR 100 is assumed to undergo a non-mechanistic tipover event at an ISFSI pad resulting in an impact with a pre-incipient impact angular velocity of ω which is readily calculated from elementary dynamics.

iii. End drop: The loaded cask is assumed to drop with its longitudinal axis in the vertical orientation such that its bottom plate hits the pad after free-falling from a height, h.

It is shown in Appendix 3.X that dynamic load factors are a function of the dominant natural frequency of vibration of the component for a given input load pulse shape. Therefore, for the purposes of this Appendix 3.A, it is desired to demonstrate that the rigid body deceleration experienced in each of the drop scenarios is below the 60g HI-STAR 100 design basis.

3.A.3 Background and Methodology

An earlier revision of this TSAR contained an analytical treatment of the three cask drop scenarios. In the earlier submittal, the cask/ISFSI interface was simulated by a linear spring with the spring stiffeners calculated using the Bousinesq elastic half-space solution. All three scenarios reduced to the solution of a simple mass-spring system. The need for such an idealized solution was eliminated when the Lawrence Livermore National Laboratory (LLNL) published results of the so-called fourth series billet tests [3.A.1] with a companion report [3.A.2] documenting a numerical solution based methodology which simulated the drop test results with reasonable accuracy. Subsequently, USNRC personnel published a paper [3.A.3] affirming the NRC's endorsement of the LLNL methodology. The LLNL simulation used modeling and simulation algorithms contained within the commercial computer code DYNA3D [3.A.6].

The LLNL cask drop model is not completely set forth in the above-mentioned LLNL reports. Using the essential information provided by the LLNL [3.A.2] report, however, Holtec is able to develop a finite element model for implementation on DYNA3D which is fully consistent with LLNL's (including the use of the Butterworth filter for discerning rigid body deceleration from "noisy" impact data). The details of the DYNA3D dynamic model, henceforth referred to as the Holtec model, are contained in the proprietary benchmark report [3.A.4] wherein it is shown that the peak

deceleration in *every* case of billet drop analyzed by LLNL is replicated within a small tolerance by the Holtec model. The case of the so-called "generic" cask for which LLNL provided predicted response under side drop and tipover events is also bounded by the Holtec model. In summary, the benchmarking effort documented in [3.A.4] is in full compliance with the guidance of the Commission [3.A.3].

Having developed and benchmarked an LLNL-consistent cask impact model, this model is applied to prognosticate the HI-STAR drop scenarios.

In the tipover scenario, the angular velocity of approach is readily calculated using planar rigid body dynamics and is used as an initial condition in the DYNA3D simulation.

For the side drop and end drop scenarios, considering the reference target (pad) elasto-plastic-damage characteristics, the object is to determine the maximum allowable drop height "h" such that the rigid body deceleration is below the design basis.

It is recognized, from the elementary analogy of the spring-mass impact, that the maximum deceleration increases monotonically as the rigidity of the cask is increased. Therefore, an upper bound on the deceleration of HI-STAR is obtained by replacing the polymeric zone in HI-STAR also by a rigid medium, making the entire cask a rigid body. Simulations for side drop and tipover conditions under the complete rigid body assumption provide an upper bound on the cask response. For the case of vertical drop, the impacting region is bottom plate forging which, without excessive conservatism, can be also modeled as a rigid body. Thus, all drop simulations presented in this appendix assume the HI-STAR 100 cask to simulate a rigid body for conservatism.

A description of the work effort and a summary of the results are presented in the following sections. In all cases, the reported decelerations are below the design basis *limit* of 60 g's *at the top of the fuel basket.*

3.A.4 Assumptions and Input Data

3.A.4.1 Assumptions

The assumptions used to create the model are completely described in Reference [3.A.4] and are shown there to be consistent with the LLNL simulation. There are two key aspects which are restated here:

The maximum deceleration experienced by the cask during a collision event is a direct function of the structural rigidity (or conversely, compliance) of the impact surface. The compliance of the ISFSI pad is quite obviously dependent on the thickness of the pad, t_p, the compressive strength of the concrete, f_c' and stiffness of the subgrade (expressed by its effective Young's modulus, E). The structural rigidity of the ISFSI pad will increase if any of the three above-mentioned parameters, t_p, f_c' or E is increased. For the reference pad, the governing parameters (i.e., t_p, f_c' and E) are

assumed to be identical to the pad defined by LLNL [3.A.2] which is also the same as the pad utilized in the benchmark report [3.A.4]. We refer to the LLNL ISFSI pad parameters as Set A. (Table 3.A.1). As can be seen from Table 3.A.1, the nominal compressive strength f_c' in Set A is limited to 4200 psi. However, experience has shown that ISFSI owners have considerable practical difficulty in limiting the 28 day strength of poured concrete to 4200 psi, chiefly because a principal element of progress in reinforced concrete materials technology has been in realizing ever increasing concrete nominal strength. Inasmuch as a key objective of the ISFSI pad is to limit its structural rigidity (and not f_c' per se), and limiting f_c' to 4200 psi may be problematic in certain cases, an alternative set of reference pad parameters is defined (Set B in Table 3.A.1) which permits a higher value of f_c' but much smaller values of pad thickness, t_p and sub-grade Young's modulus, E. The ISFSI owner has the option of constructing the pad to comply with the limits of Set A or Set B without performing site-specific cask impact analyses. It is recognized that, for a specific ISFSI site, the reinforced concrete, as well as the underlying engineered fill properties, may be different at different locations on the pad or may be uniform, but non-compliant with either Set A or Set B. In that case, the site-specific conditions must be performed to demonstrate compliance with the design limits of the HI-STAR system (e.g., maximum rigid body g-load less than or equal to 60g's). The essential data which define the pad (set A and set B) used to qualify the HI-STAR 100 are provided in Table 3.A.1.

As the results presented in this appendix show, Set B parameters lead to a lower g-loads than the LLNL Set (Set A).

3.A.4.2 Input Data

Table 3.A.1 characterizes the properties of the reference target pad *(Set A and Set B)* used in the analysis.

The principal strength parameters that define the stiffness of the pad, namely t_p, E and f_c' are input in the manner described in [3.A.2] and [3.A.4].

Table 3.A.2 details the geometry of the HI-STAR 100 used in the drop simulations. This data is taken from applicable HI-STAR 100 drawings.

3.A.5 Finite Element Model

The finite-element model of the Holtec HI-STAR 100 cask (bottom plate, shells, forging, lid, Holtite polymer and its connectors), concrete pad and a portion of the subgrade soil is constructed using the pre-processor integrated with the LS-DYNA3D software [3.A.5]. The deformation field for all postulated drop events, the end-drop, the side-drop and the tipover, exhibits symmetry with the vertical plane passing through the vertical diameter of the cask and the concrete pad length. Using this symmetry condition of the deformation field a half finite-element model is constructed. The finite-element model is organized into five independent parts (the cask, the MPC steel plates, the

basket fuel zone, the concrete pad and the soil). The final model contains 35431 nodes, 29944 solid type finite-elements, five (5) materials, one (1) property and four (4) interfaces. The finite-element model used for the side-drop and tipover-drop events is depicted in Figures 3.A.1 through 3.A.4. Figures 3.A.5 through 3.A.8 show the end-drop finite-element model.

The half portion of the cylindrical cask contains 7,320 solid finite-elements. Figure 3.A.11 depicts details of the cask finite-element mesh.

The elasto-plastic behavior characteristics of all HI-STAR components (shells, lids, Holtite, outer skin, connectors, etc.) are simulated as rigid materials using a DYNA3D built-in command.

The soil grid, shown in Figure 3.A.9, is a rectangular prism (800 inches long, 375 inches wide and 470 inches deep), is constructed from 13294 solid type finite-elements. The material defining this part is an elastic orthotropic material. The central portion of the soil (400 inches long, 150 inches wide and 170 inches deep) where the stress concentration is expected to appear is discretized with a finer mesh.

The concrete pad is 320 inches long, 100 inches wide and is 36 inches thick. This part contains 8208 solid finite-elements. A uniform sized finite-element mesh, shown in Figure 3.A.10, is used to model the concrete pad. The concrete behavior is described using a special constitutive law and yielding surface contained within DYNA3D. The geometry, the material properties, and the material behavior are identical to the LLNL reference pad.

The MPC and the contained fuel is modeled in two parts which represent the lid and baseplate, and the fuel area. An elastic material is used for both parts. The finite-element mesh pertinent to the MPC contains 1122 solid finite-elements and is shown in Figure 3.A.14. The mass density is appropriate to match a representative weight of 241,937 lb which is an approximate mean of the upper and lower weight estimates for a loaded HI-STAR 100. The total weight used in the analysis is approximately 8,000 lb heavier than the HI-STAR 100 containing the lightest weight MPC.

Analysis of a single mass impacting a spring with a given initial velocity shows that both the maximum deceleration "a_M" of the mass and the time duration of contact with the spring "t_c" are related to the dropped weight "w" and drop height "h" as follows:

$$a_M \sim \frac{\sqrt{h}}{\sqrt{w}} \; ; \; t_c \sim \sqrt{w}$$

Therefore, the most conservatism is introduced into the results by using the minimum weight. However, since the difference between the heaviest and the lightest HI-STAR 100 is only 9,500 lb, a small percentage of the total weight, the results using the minimum weight will yield a 2% increase in the maximum deceleration and a 2% decrease in the duration of the impact. This small difference is neglected in the presentation of results.

It is emphasized that the finite element model described in the foregoing is identical in its approach to the "Holtec model" described in the benchmark report [3.A.4]. Gaps between the MPC and the overpack are included in the model.

3.A.6 Impact Velocity

a. Linear Velocity: Vertical Drops

For the side drop and vertical drop events, the impact velocity, v, is readily calculated from the Newtonian formula:

$$v = \sqrt{(2gh)}$$

where

g = acceleration due to gravity
h = free-fall height

b. Angular velocity: Tipover

The tipover event is an artificial construct wherein the HI-STAR 100 overpack is assumed to be perched on its edge with its C.G. directly over the pivot point A (Figure 3.A.15). In this orientation, the overpack begins its downward rotation with zero initial velocity. At angle ψ_1 (Figure 3.A.17), the pivot point shifts to point B; but otherwise the downward rotation of the overpack continues with increasing angular velocity. Towards the end of the tipover, the overpack is horizontal with its downward velocity ranging from zero at the pivot point to a maximum at the farthest point of impact (point E in Figure 3.A.18). The angular velocity at the instant of impact defines the downward velocity distribution along the contact line.

In the following, we derive an explicit expression for calculating the angular velocity of the cask at the instant when it impacts on the ISFSI pad.

Referring to Figure 3.A.15, let r be the length AC where C is the cask centroid. Therefore,

$$r = \left(\frac{d^2}{4} + (h+a)^2 \right)^{1/2} \qquad \textbf{(3.A.1)}$$

The mass moment of inertia of the HI-STAR 100 System, considered as a rigid body, can be written about an axis through point A, as

$$6I_A = I_c + \frac{W}{g} r^2 \qquad \textbf{(3.A.2)}$$

where I_c is the mass moment of inertia about a parallel axis through the cask centroid C, and W is the weight of the cask (W = Mg).

Let $\theta_1(t)$ be the rotation angle between a vertical line and the line AC. The equation of motion for rotation of the cask around point A, during the time interval prior to contact with point B (Figure 3.A.15), is

$$I_A \frac{d^2 \theta_1}{dt^2} = Mgr \sin \theta_1 \qquad \textbf{(3.A.3)}$$

This equation can be rewritten in the form

$$\frac{I_A}{2} \frac{d (\dot{\theta}_1)^2}{d \theta_1} = Mgr \sin \theta_1 \qquad \textbf{(3.A.4)}$$

which can be integrated over the limits $\theta_1 = 0$ to $\theta_1 = \psi_1$. (See Figure 3.A.17).

The final angular velocity θ_1 at the time instant just prior to contact at point B is given by the expression

$$\dot{\theta}_1 (t_B) = \sqrt{\frac{2\ Mgr}{I_A} (1 - \cos \psi_1)} \qquad \textbf{(3.A.5)}$$

The angle ψ_1 between AC and the vertical, at the time just prior to contact, is given by geometry as

$$\psi_1 = \psi_A - \psi_B \qquad \textbf{(3.A.6)}$$

where

$$\psi_A = \tan^{-1} \left(\frac{a}{b}\right)$$

$$\psi_B = \tan^{-1} \left(\frac{d}{2h}\right)$$

and a and b are shown in Figure 3.A.17. At contact with point B at time t_B (Figure 3.A.16), the angular impulse momentum equation can be used to determine a new initial angular velocity for subsequent determination of the angular motion about point B. Ignoring the small impulsive moment

from the cask weight due to the instantaneous change in moment arm, the angular momentum balance gives

$$I_A \dot{\theta}_1 (t_B) = I_B \dot{\theta}_2 (0) \qquad \textbf{(3.A.7)}$$

where $I_B = I_C + Mr_1^2$ is the mass moment of inertia of the cask about point B. Solving for θ_2 (0) and eliminating θ_1 (t_b) using Eq. (3.A.5) gives

$$\dot{\theta}_2(0) = \sqrt{\frac{2\, Mg\, r_1}{I_B} \frac{I_A}{I_B} (1 - \cos \psi_1) (\frac{r}{r_1})} \qquad \textbf{(3.A.8)}$$

The angle $\theta_2(0)$, which is the starting point for the rotational motion around point B, is easily obtained from the cask geometry. With X defined in Figure 3.A.16.

$$\sin\theta_2(0) = \frac{X(0)}{r_1} \qquad \textbf{(3.A.9)}$$

where X(0) can be determined from Figure 3.A.17 as

$$X(0) = r \sin \psi_1 - (a^2 + b^2)^{1/2}$$

so that

$$\sin\theta_2(0) = \frac{r}{r_1} \sin \psi_1 - \frac{(a^2 + b^2)^{1/2}}{r_1} \qquad \textbf{(3.A.10)}$$

where

$$r_1 = \left[(\frac{D}{2})^2 + h^2 \right]^{1/2}$$

With the initial conditions determined by Eq. (3.A.9) and (3.A.10), the solution for the motion $\theta_2(t) \geq \theta_2(0)$ is easily obtained.

The angular velocity θ_{2f} at the instant of ground contact is

$$\dot{\theta}_{2f}^2 - \dot{\theta}_2^2(0) = \frac{2\ Mgr_1}{I_B}\left(\cos\ \theta_2(0) - \cos\ \theta_{2f}\right) \qquad \textbf{(3.A.11)}$$

where, from Figure 3.A.18

$$\theta_{2f} = \cos^{-1}\left(\frac{D}{2r_1}\right) \qquad \textbf{(3.A.12)}$$

Using Eq. (3.A.8) to eliminate θ_2 (0) from Eq. (3.A.11) leads to a solution for the angular velocity θ_{2f} when interface contact occurs, in the form

$$\dot{\theta}_{2f} = \sqrt{\frac{2Mgr_1}{I_B}\ \beta} = \omega \qquad \textbf{(3.A.13)}$$

$$where\ \beta = \frac{I_A r}{I_B\ r_1}\ (1 - \cos\ \psi_1) + \cos\ \theta_2(0) - \cos\ \theta_{2f} \qquad \textbf{(3.A.14)}$$

Equations (3.A.13) and (3.A.14) establish the initial conditions for the final phase of the tipover analysis; namely, the portion of the motion when the cask is decelerated by the resistive force at the ISFSI pad interface.

Using the data germane to HI-STAR 100 (Table 3.A.2), and the above equations, the angular velocity of impact is calculated as 1.79 rad/sec.

3.A.7 Results

3.A.7.1 Set A Pad Parameters:

The LS-DYNA3D time-history results are processed using the Butterworth filter (in conformance with the LLNL methodology) to establish the time-history rigid body motion of the cask. The material points on the cask where the acceleration displacement and velocity are computed for each of the three drop scenarios are shown in Figure 3.A.19.

Node 2901 (Channel A2), which is located midway on the outermost shell generator at the top in side drop events serves as the reference point.

Node 5151 (Channel A1), which is located at the center of the outer surface of the bottom forging, serves as the reference point for end-drop scenarios.

Node 6000 (Channel A3), which is located at the center of the cask top lid outer surface, serves as the reference point for the tipover scenario with the pivot point indicated as Point 0 in Figure 3.A.19.

The results reported below for maximum cask-ISFSI contact force have been multiplied by 2.0 to reflect the fact that only 50% of the dropped mass is included in the model due to the symmetry assumption.

i. Side Drop:

~~Figures 3.A.20-3.A.23, respectively, show~~ *T*he time-histories of the impact force and displacement, velocity, and deceleration at the reference node point (Channel A2) *have been determined for a* drop height, ~~is~~ h, *of* 72". Using the data from Figure 3.A.20, the peak cask/pad impact force is 9.636E+06 lbs and the contact duration associated with the initial peak is 9.5 milli-seconds.

The maximum rigid body deceleration (filtered at 350 Hz cut-off frequency) ~~as shown in Figure 3.A.23~~ is 49.67 g's, ~~value~~ which is below the design basis limit of 60 g's. The time duration of the peak deceleration pulse is 4.4 milli-seconds.

ii. Tipover:

Figures 3.A.24-3.A.27, respectively, show the time-histories of the impact force and displacement, velocity and vertical deceleration of Channel A3 (in Figure 3.A.19) for this event.

The deceleration at the tip of the fuel basket is obtained by ratioing the filtered deceleration of Node 6000. The maximum filtered deceleration at the tip of the fuel basket is ~~found from Figure 3.A.27 to be~~ 66.02 x 0.906 = 59.81 g's which is below the design basis limit. The 0.906 multiplier is based on the geometry of the loaded HI-STAR 100 (further explained in Table 3.A.3). The maximum contact force in this event is 6.43E+06 lbs and the contact duration associated with the initial peak is approximately 8.8 milli-seconds. It should be emphasized that the calculated deceleration for Node 6000 was filtered at 350 Hz cut-off frequency.

The duration of the initial deceleration pulse is ~~obtained from Fig. 3.A.27 as~~ 4.4 milli-seconds.

iii. End Drop:

As in all other impact cases analyzed in this appendix, the overpack is treated as a completely rigid body in the end drop scenario. One drop height is considered: h = 21". The results are summarized in Table 3.A.3 and ~~Figures 3.A.28-3.A.31, respectively, show~~ the contact force, displacement, velocity, and acceleration time-histories at Channel A1 ~~(Figure 3.A.19)~~ for the 21" end drop *are documented in the calculation package*. The duration of the contact force initial pulse is approximately 2.7 milli-seconds, and the filtered cask deceleration pulse is 2.1 milli-seconds.

A carry height of 21" gives peak filtered deceleration in the event of an end drop of approximately 53 g's.

Decelerations obtained from the DYNA3D numerical solutions are filtered through a Butterworth type filter identical to the filter used by LLNL to investigate the "generic" cask [3.A.2]. The filter has the following characteristics: 350 Hz passband frequency, 10,000 Hz stopband frequency, 0.15 maximum passband ripple, and 10 minimum stopband attenuation.

The computer code utilized in this analysis is LS-DYNA3D [3.A.5] validated under Holtec's QA system. *Table 3.A.3 summarizes the key results for all impact simulations for the Set A parameters discussed in the foregoing.*

3.A.7.2 Set B pad Parameters:

As stated previously, Set B parameters produce a much more compliant pad than the LLNL reference pad (Set A). This fact is borne out by the side drop, tipover and end drop analyses performed on the pad defined by the Set B parameters. Table 3.A.4 provides the filtered results for the three impact scenarios. In every case, the peak decelerations corresponding to Set B parameters are less than those for Set A (provided in Table 3.A.3).

Impact force and acceleration time history curves for Set B have the same general shape as those for Set A and are contained in the calculation package. All significant results are summarized in Table 3.A.4.

3.A.8 Computer Codes and Archival Information

The input and output files created to perform the analyses reported in this appendix are archived in the Holtec International calculation package.

3.A.9 Conclusion

The DYNA3D analysis of HI-STAR 100 reported in this appendix leads to the following conclusion:

a. If a loaded HI-STAR undergoes a free fall for a height of 21 inches in a vertical orientation, the maximum rigid body deceleration is limited to 52.26 g's and 50.25 g's for Set A and Set B pad parameters, respectively.

b. If a loaded HI-STAR 100 undergoes a free fall in a horizontal orientation (side drop) for a height 72", the maximum rigid body deceleration is limited to 49.67 and 46.77g's for Set A and Set B pad parameters, respectively.

c. If a loaded HI-STAR 100 overpack pivots about its bottom edge and tips over then the maximum rigid body deceleration of the cask centerline at the plane of the top of the fuel basket cellular region is 59.81 and 50.64 g's respectively for pad parameter Set A and Set B.

Tables 3.A.3 and 3.A.4 provides the key results for all drop cases studied herein for pad parameter Set A and B respectively.

Recalling that the design basis g-load is 60 g's, the above impact scenarios are comfortably enveloped by the level D design limit and allow ample margin for the introduction of appropriate dynamic load factors into the component stress analyses.

If the pad designer maintains each of the three significant parameters (t_p, f_c' and E) below the limit for the specific set selected (Set A or Set B), then the stiffness of the pad at the ISFSI site will be lower and the computed decelerations at the ISFSI site will also be expected to be lower. Furthermore, because the mathematical model for the cask assumes infinite rigidity (which is not a requirement for the LLNL methodology (3.A.2) or Holtec's benchmark work effort (3.A.4), refinement of the cask dynamic model will accrue further reduction in the computed peak deceleration. Likewise, incorporation of the structure flexibility in the MPC enclosure vessel, fuel basket, etc., would lead to additional reductions in the computed values of the peak deceleration. These refinements, however, add to the computational complexity. Because g-limits are met without the above-mentioned and other refinements in the cask dynamic model, the rigid body model for HI-STAR 100 was retained to preserve simplicity.

3.A.10 References

[3.A.1] Witte, M., et al., "Evaluation of Low-Velocity Impacts Tests of Solid Steel Billet onto Concrete Pads.", Lawrence Livermore National Laboratory, UCRL-ID-126274, Livermore, California, March 1997.

[3.A.2] Witte, M., et al., "Evaluation of Low-Velocity Impacts Tests of Solid Steel Billet onto Concrete Pads, and Application to Generic ISFSI Storage Cask for Tipover and Side Drop.", Lawrence Livermore National Laboratory, UCRL-ID-126295, Livermore, California, March 1997.

[3.A.3] Tang, D.T., Raddatz, M.G., and Sturz, F.C., "NRC Staff Technical Approach for Spent Fuel Cask Drop and Tipover Accident Analysis", SFPO, USNRC (1997).

[3.A.4] Simulescu, I., "Benchmarking of the Holtec LS-DYNA3D Model for Cask Drop Events", Holtec Report HI-971779, September 1997.

[3.A.5] LS-DYNA3D, Version 936-03, Livermore Software Technology Corporation, September 1996.

[3.A.6] Whirley, R.G., "DYNA3D, A Nonlinear, Explicit, Three-Dimensional Finite element Code for Solid and Structural Mechanics - User Manual.", Lawrence Livermore National Laboratory, UCRL-MA-107254, Revision 1, 1993.

[3.A.6] Zhai, J. "Analysis of the Loaded HI-STAR 100 System Under Drop and Tip-Over Scenarios, Holtec Report HI-2002466.

Table 3.A.1: Essential Variables to Characterize the ISFSI Pad *(Set A and Set B)*

Item	*Parameter Set A*	*Parameter Set B*
Thickness of concrete (inches)	*36*	*28*
Nominal compressive strength of concrete (psi)	*4,200*	*6,000*
Max. Modulus of elasticity of the subgrade (psi)	*28,000*	*16,000*

Notes:

1. The concrete Young's Modulus is derived from the American Concrete Institute recommended formula $57{,}000\sqrt{f}$ where f is the nominal compressive strength of the concrete (psi).

2. *The effective modulus of elasticity of the subgrade shall be measured by the classical "plate test" or other appropriate means before pouring of the concrete to construct the ISFSI pad.*

Table 3.A.2: Key Input Data in Drop Analyses

Cask weight	128,275 lb
Holtite weight	12,926 lb
Holtite connectors weight	11,879 lb
Length of the cask	203.125 inches
Length of the Holtite	173.125 inches
Diameter of the bottom plate	83.25 inches
Inside diameter of the cask	68.75 inches
Outside diameter of the cask shells	85.75 inches
Outside diameter of the enclosure plate	96.00 inches
Outside diameter of the Holtite	95.00 inches
MPC weight (including fuel)	88,857 lb
MPC height	190.5 inches
MPC diameter	68.375 inches
MPC bottom plate thickness	2.5 inches
MPC top plate thickness	9.5 inches

Table 3.A.3: FILTERED RESULTS FOR DROP AND TIPOVER SCENARIOS *(SET A)*

Drop Event	Rigid Cask Model†			
	Max. Displ (in)	**Impact Velocity (in/sec)**	**Max. Acc. (g's)**	**Acc. Pulse Duration (msec.)**
End-21"	1.144	127.4	52.26	2.1
Side-72"	2.674	235.9	49.67	4.4
Tipover Top of Cask††	4.231	348.4	66.02	4.4
Tipover Top of Basket Elevation	--	--	59.81	--

† The passband frequency of the Butterworth filter is 350 Hz.

†† The distance of the top of the fuel basket is 176.25" from the pivot point. The distance of the top of the cask is 194.375" from the pivot point. Therefore, all displacements, velocities, and accelerations of the top of the basket are 90.6% of the cask top (176.25/194.4).

Table 3.A.4: FILTERED RESULTS FOR DROP AND TIPOVER SCENARIOS (SET B)

	Rigid Cask Model†			
Drop Event	***Max. Displ (in)***	***Impact Velocity (in/sec)***	***Max. Acc. (g's)***	***Acc. Pulse Duration (msec.)***
End-21"	*1.335*	*127.4*	*50.25*	*2.0*
Side-72	*4.533*	*235.9*	*46.77*	*4.0*
Tipover Top of Cask††	*6.620*	*348.4*	*55.89*	*4.0*
Tipover Top of Basket Elevation	--	--	*50.64*	--

† The passband frequency of the Butterworth filter is 350 Hz.

†† The distance of the top of the fuel basket is 176.25" from the pivot point. The distance of the top of the cask is 194.375" from the pivot point. Therefore, all displacements, velocities, and accelerations of the top of the basket are 90.6% of the cask top (176.25/194.4).

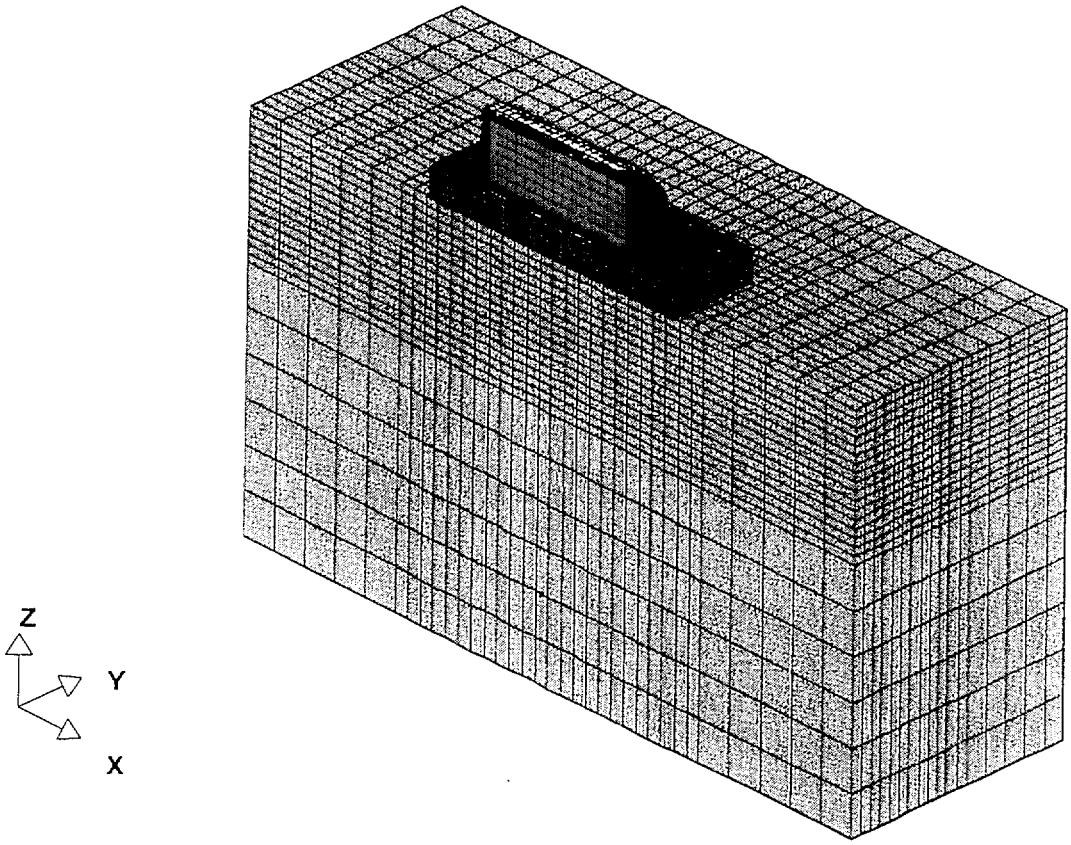

Fig. 3.A.1 Side-Drop and Tipover Finite-Element Model (3-D View)

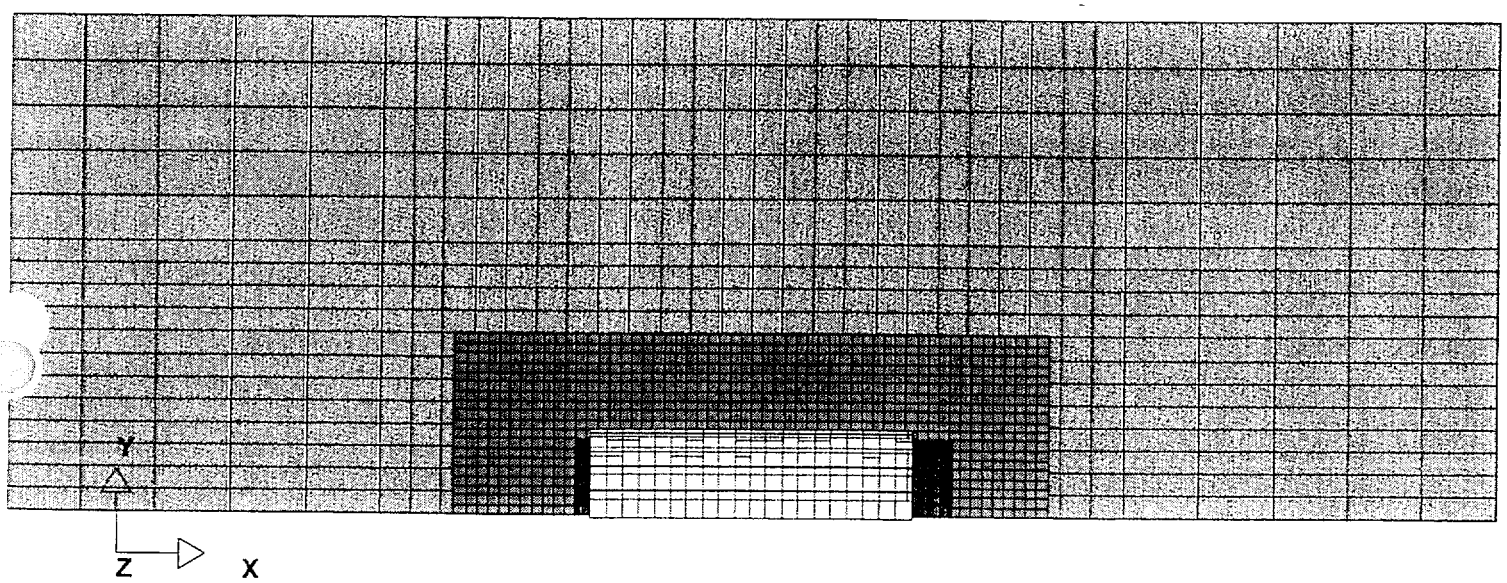

Fig. 3.A.2 Side-Drop and Tipover Finite-Element Model (Plan View)

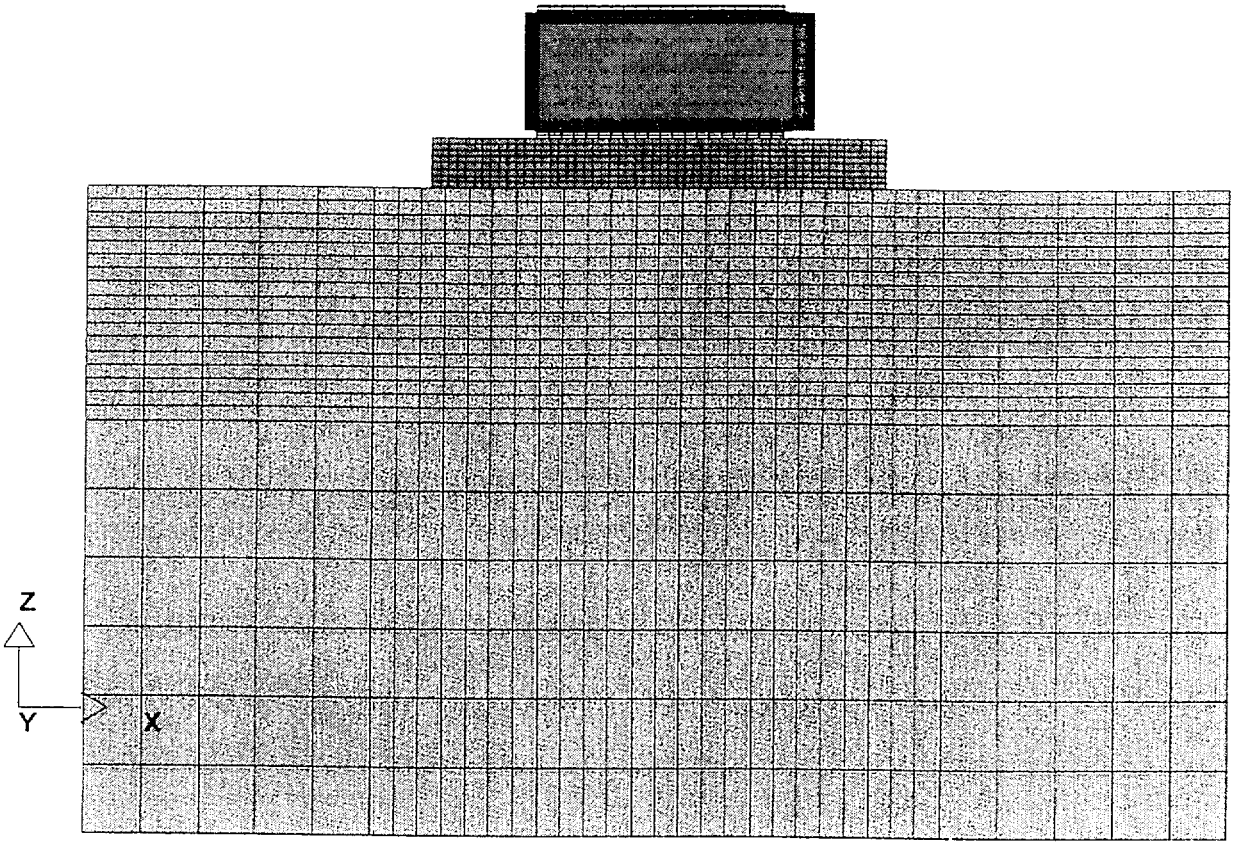

Fig. 3.A.3 Side-Drop and Tipover Finite-Element Model (XZ View)

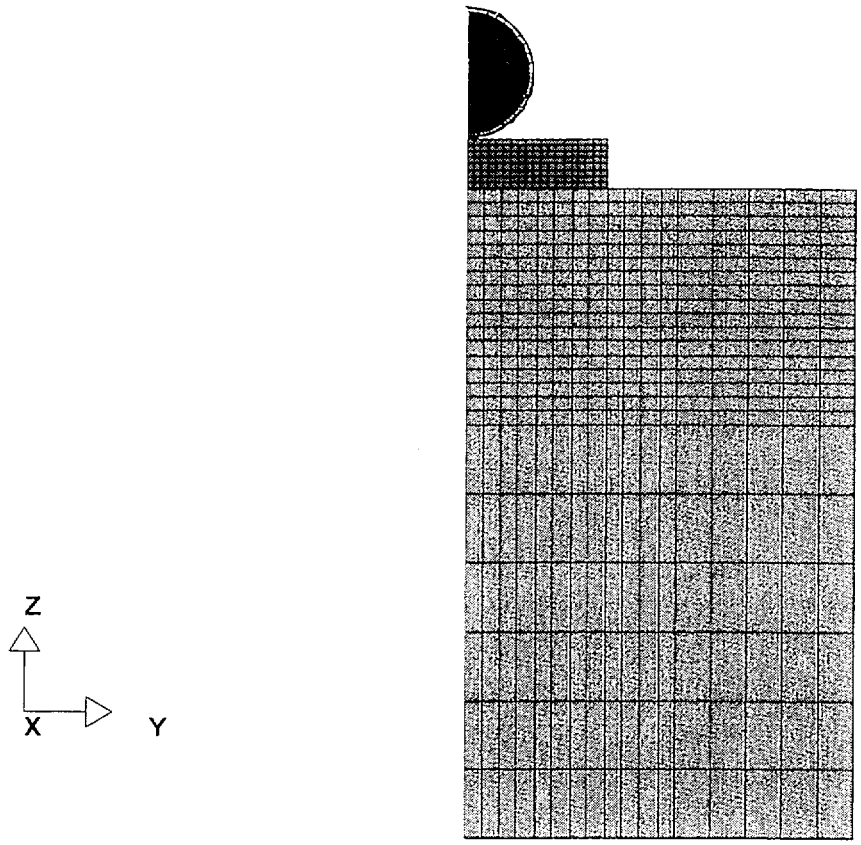

Fig. 3.A.4 Side-Drop and Tipover Finite-Element Model (YZ View)

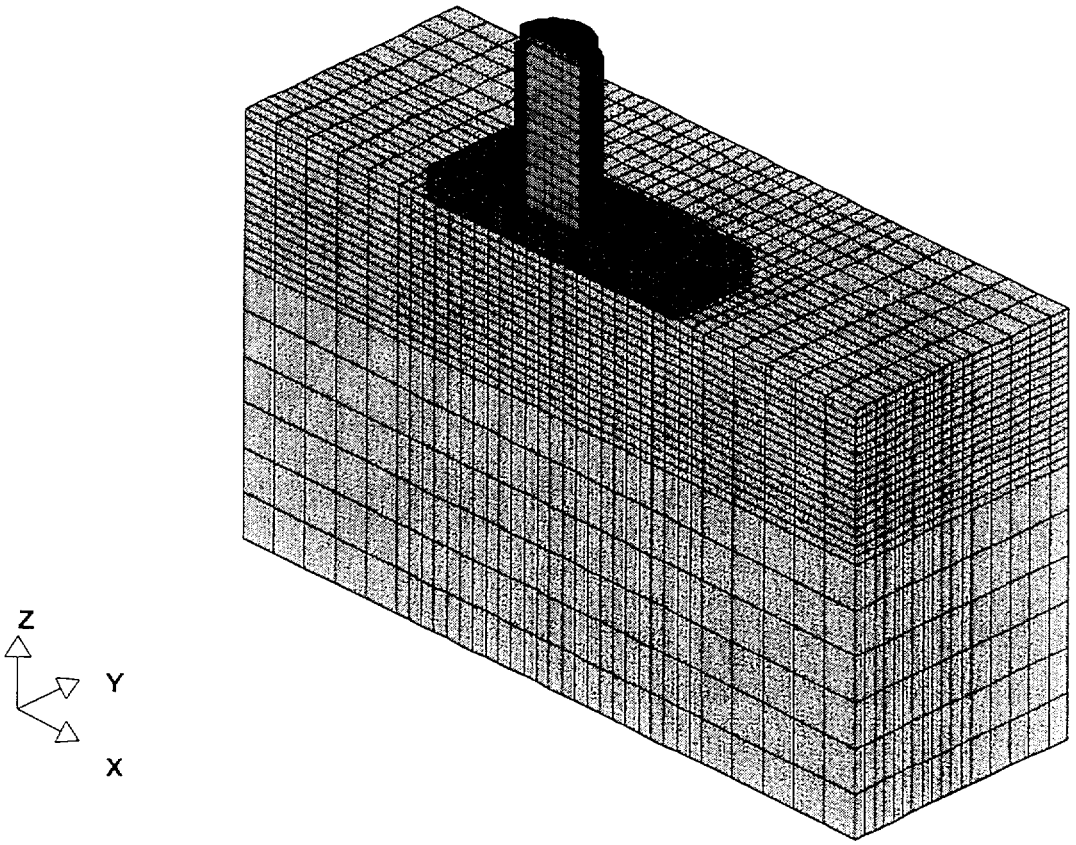

Fig. 3.A.5 End-Drop Finite-Element Model (3-D View)

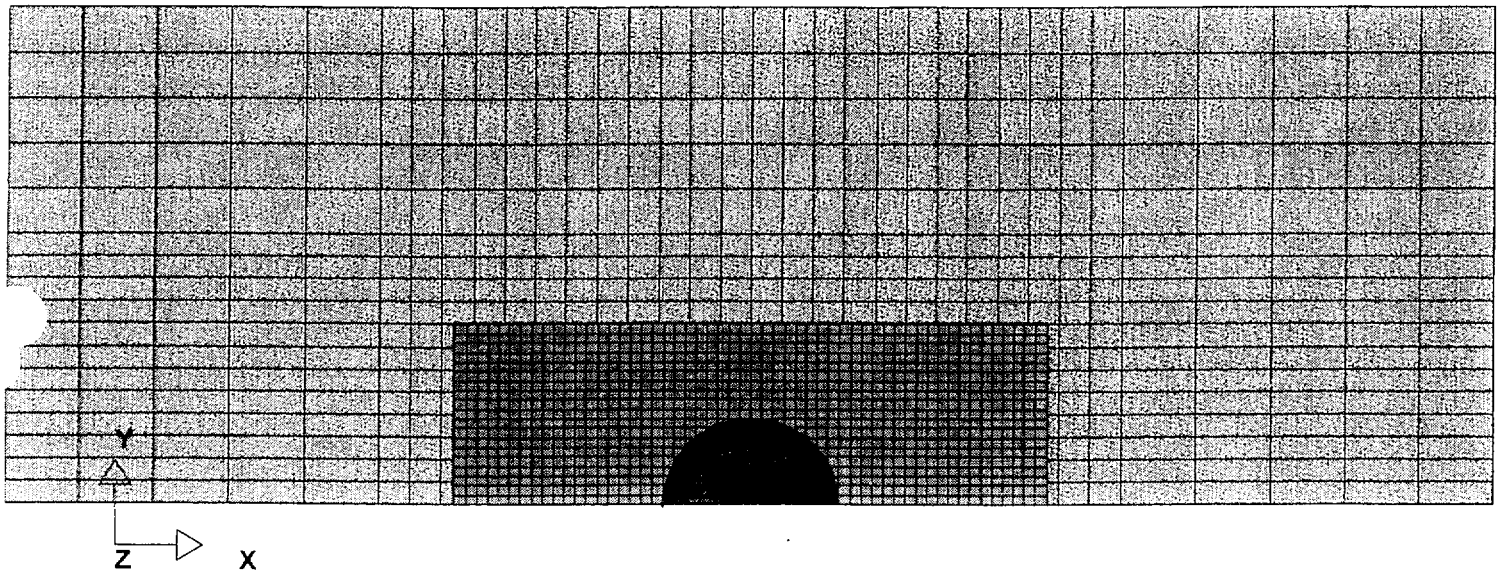

Fig. 3.A.6 End-Drop Finite-Element Model (Plan View)

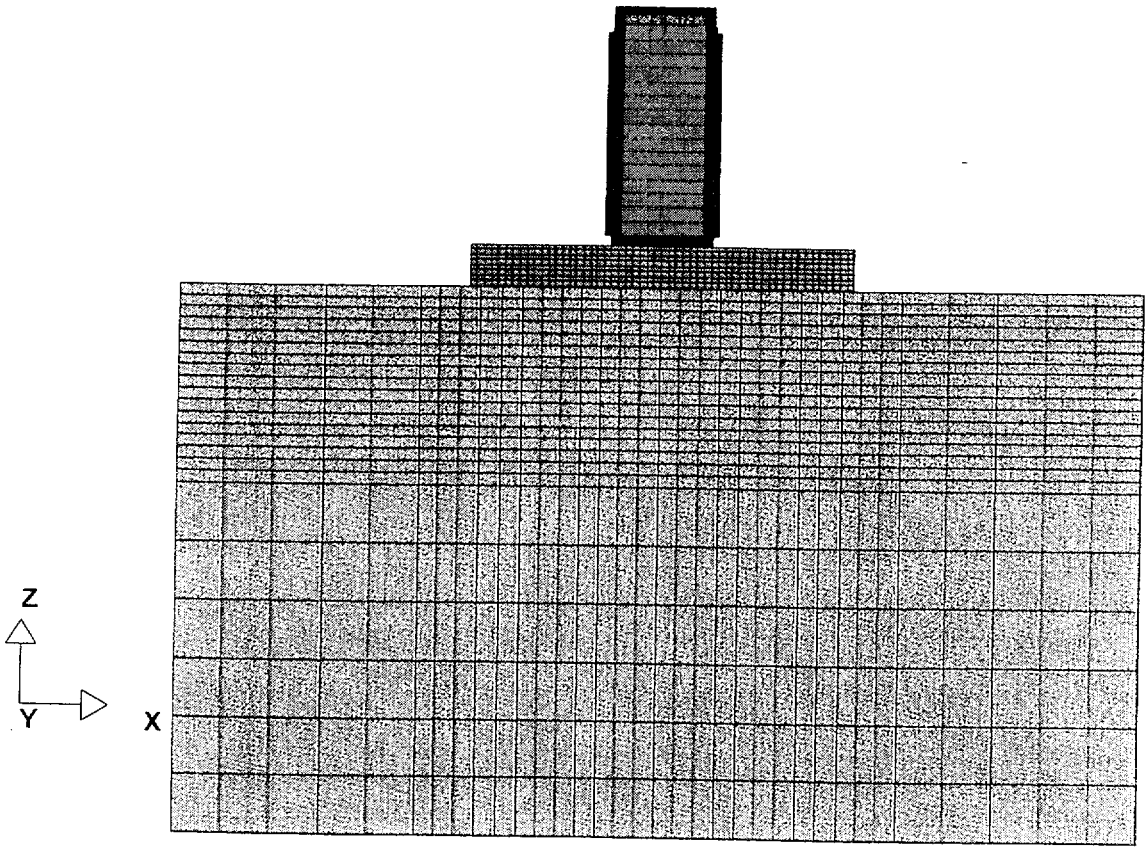

Fig. 3.A.7 End-Drop Finite-Element Model (XZ View)

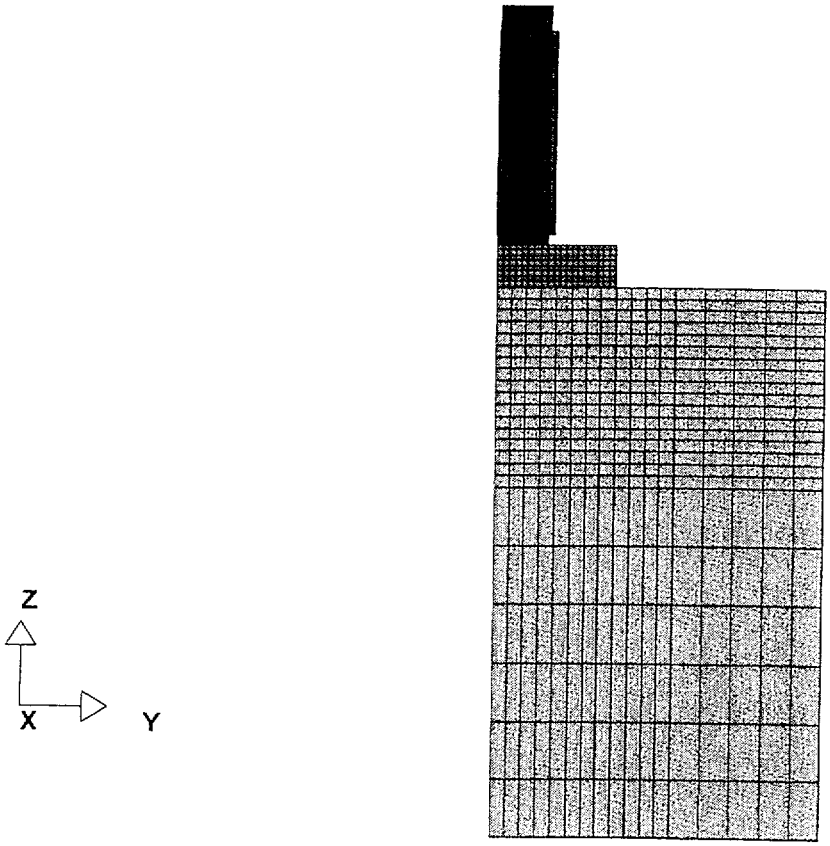

Fig. 3.A.8 End-Drop Finite-Element Model (YZ View)

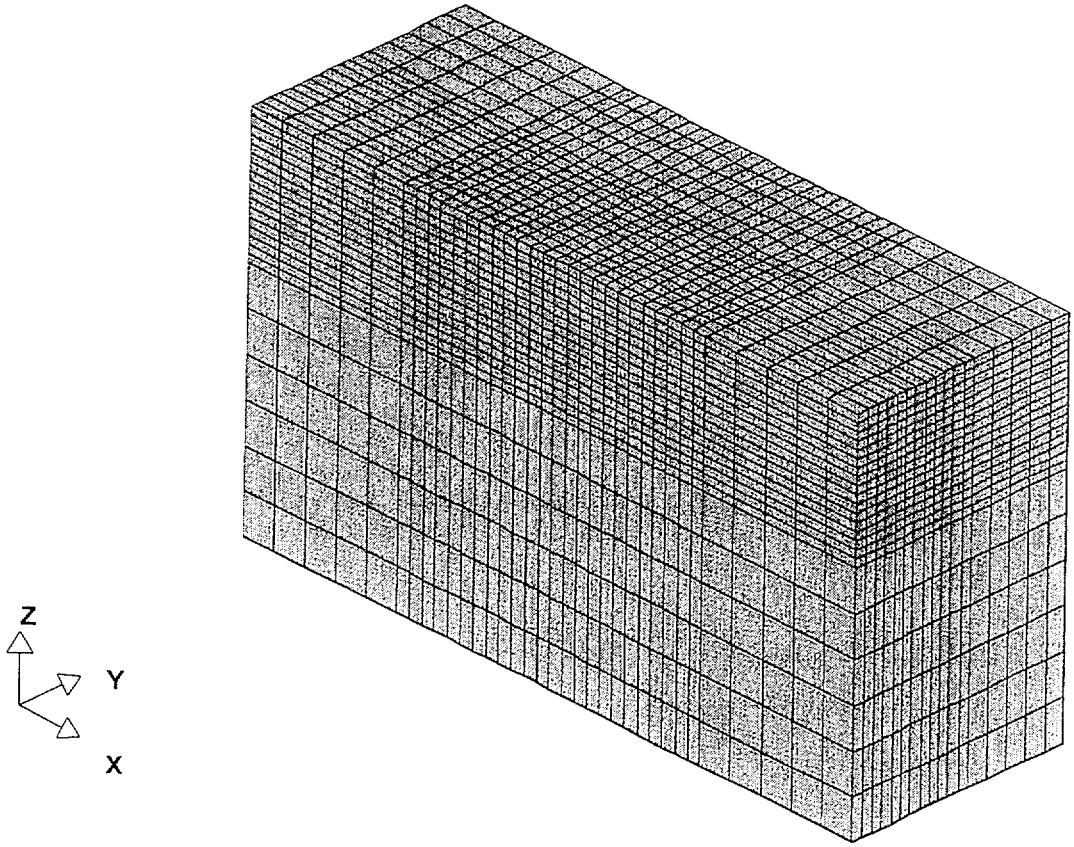

Fig. 3.A.9 Soil Finite-Element Model (3-D View)

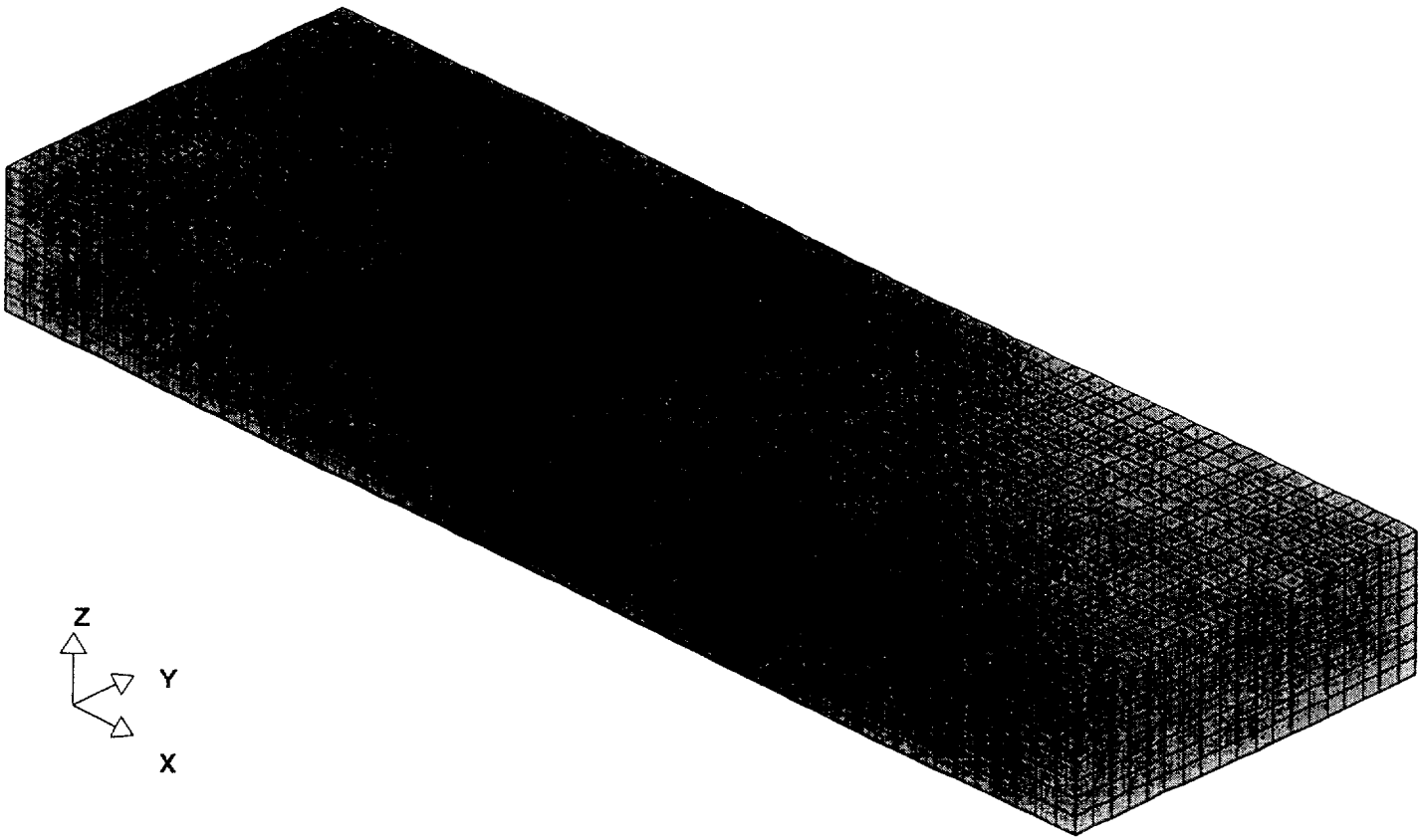

Fig. 3.A.10 Concrete Pad Finite-Element Model (3-D View)

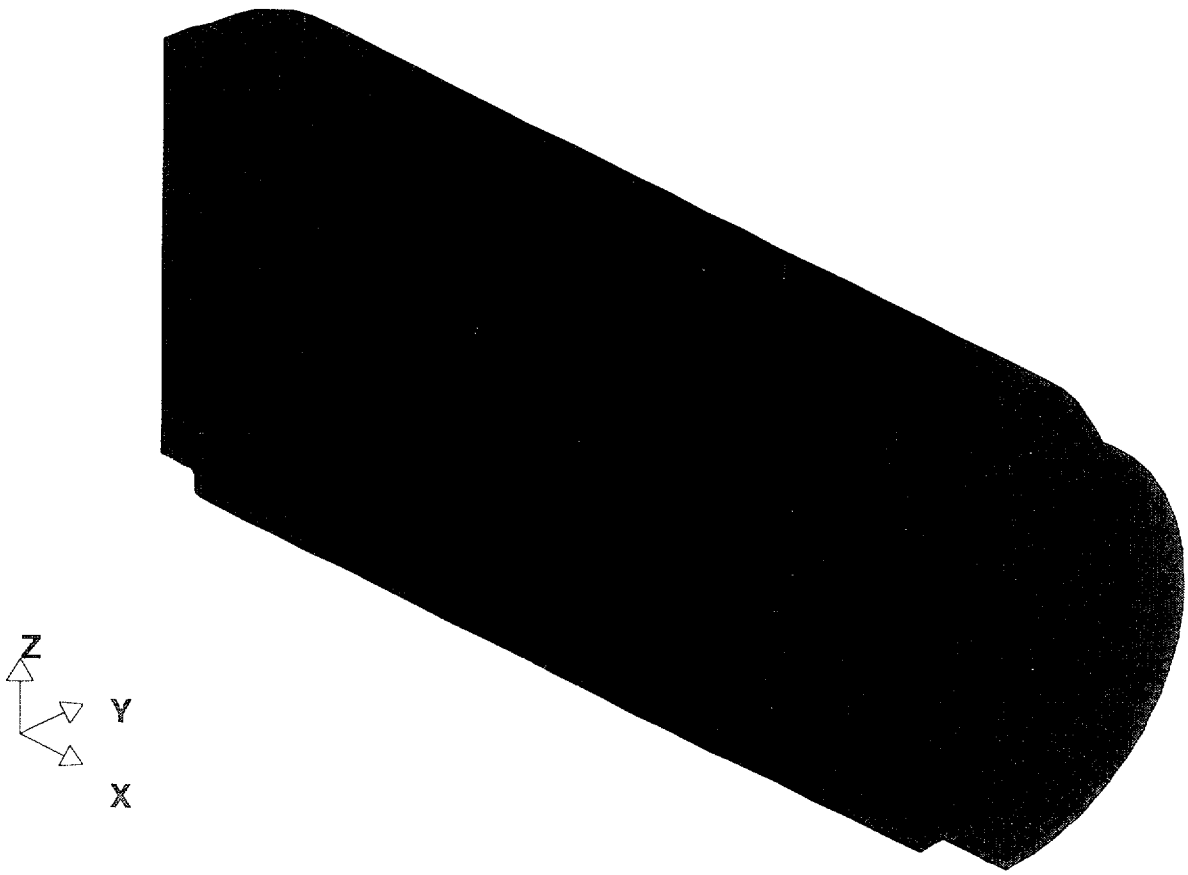

Figure 3.A.ll Cask Finite-Element Model (3-D View)

Wed Nov 11 16:14:27 1993
KBS2 LSDyna3d PrePost

FIGURE 3.A.12 DELETED

FIGURE 3.A.13 DELETED

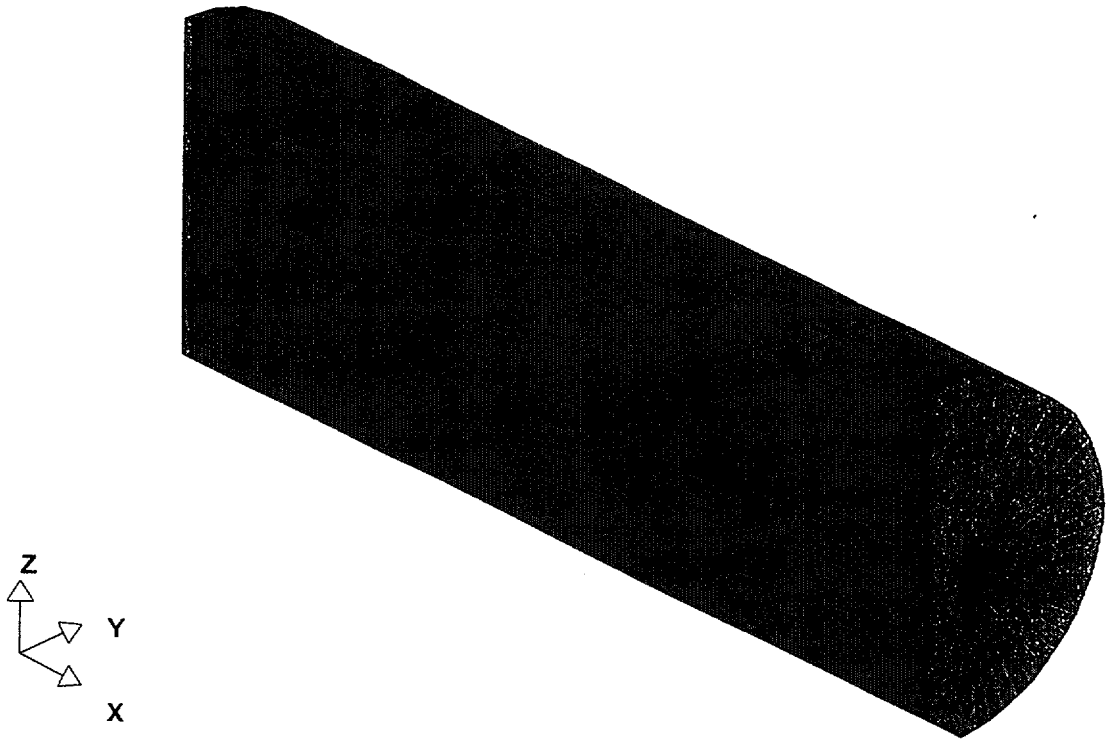

Fig. 3.A.14 MPC Finite-Element Model (3-D View)

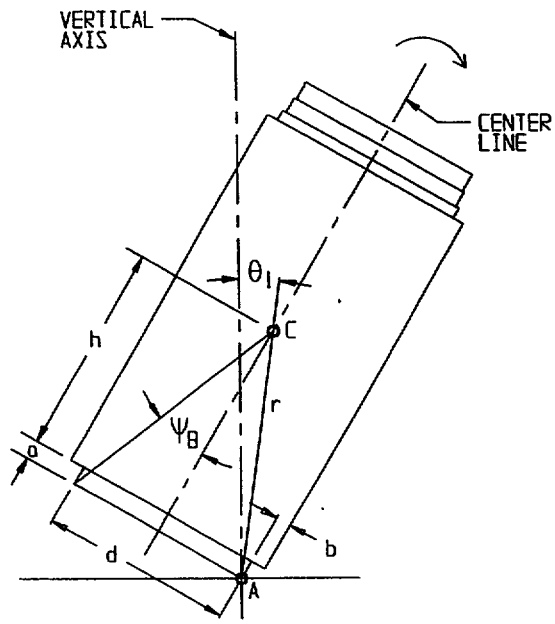

FIGURE 3.A.15; PIVOT POINT SHIFT DURING TIP-OVER INITIAL CONDITION

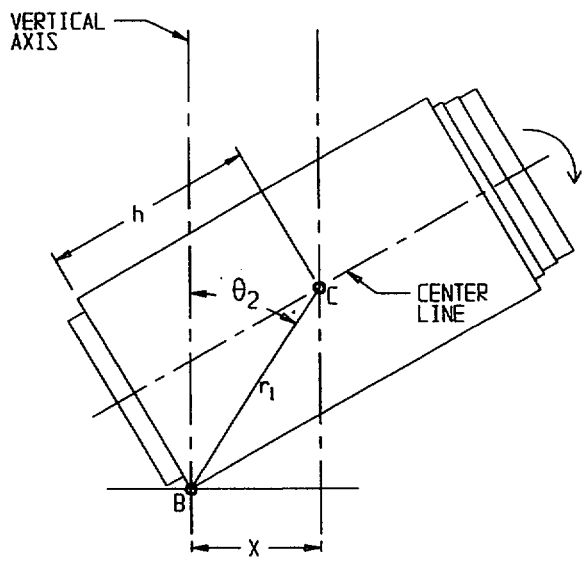

FIGURE 3.A.16; PIVOT POINT SHIFT DURING TIP-OVER INTERMEDIATE CONDITION

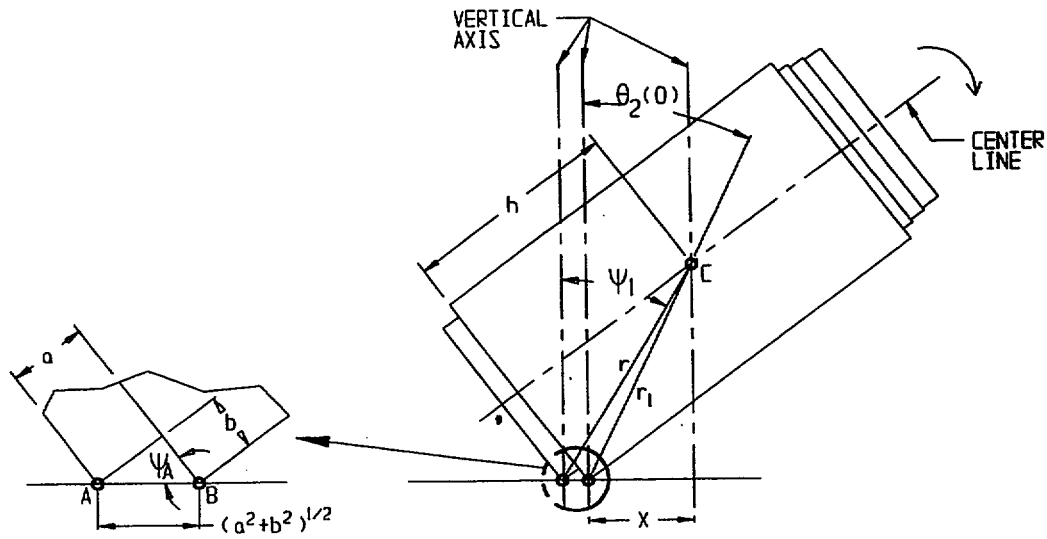

FIGURE 3.A.17; TIP-OVER EVENT AT THE INSTANT WHEN POINTS A AND B ARE BOTH IN CONTACT WITH THE GROUND

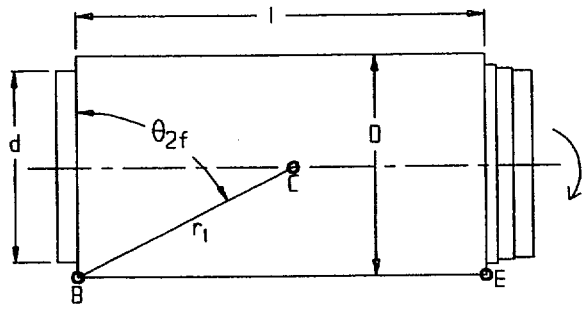

FIGURE 3.A.18; TIP-OVER EVENT OVERPACK SLAMS AGAINST THE FOUNDATION DEVELOPING A RESISTIVE FORCE

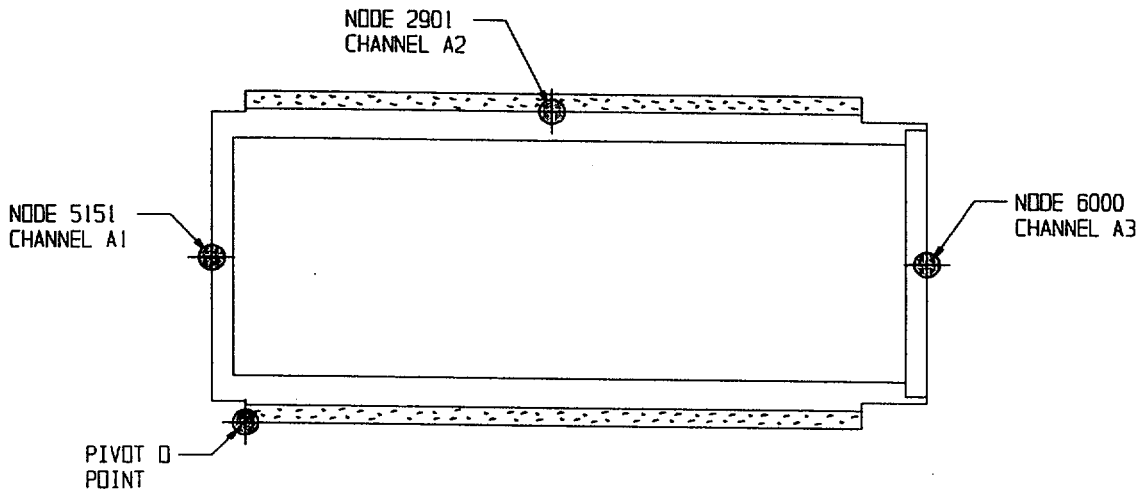

FIGURE 3.A.19; MEASUREMENT POINTS AND CORRESPONDING FINITE-ELEMENT MODEL NODES